# Powder X-ray diffraction of tafamidis Form 1, $C_{14}H_7Cl_2NO_3$

Tawnee M. Ens[1], James Kaduk[1,2], Anja Dosen[3] and Tom Blanton[3]
[1]North Central College, 131 South Loomis Street, Naperville, IL 60540, USA
[2]Illinois Institute of Technology, 3101 South Dearborn Street, Chicago, IL 60616, USA
[3]International Centre for Diffraction Data (ICDD), 12 Campus Boulevard, Newtown Square, PA 19073-3273, USA

(Received 14 April 2025; revised 18 July 2025; accepted 23 July 2025)

Abstract: The crystal structure of tafamidis has been independently resolved and refined using synchrotron X-ray powder diffraction data and optimized using density functional techniques. Tafamidis crystallizes in space group $P2_1/c$ (#14) with $a$ = 3.787093(6), $b$ = 14.97910(4), $c$ = 22.93751(7) Å, $\beta$ = 90.92672(19)°, $V$ = 1,301.012(4) Å$^3$, and $Z$ = 4 at 295 K. The crystal structure consists of stacks of molecules along the $a$-axis. The molecules are inclined to this axis; the mean plane is (−4, 2, 11). Strong centrosymmetric O–H···O hydrogen bonds exist between carboxylic acid groups. The molecules are linked along the $b$-axis by C–H···N hydrogen bonds. Two C–H···Cl hydrogen bonds also contribute to the lattice energy. The powder pattern has been submitted to the International Centre for Diffraction Data for inclusion in the Powder Diffraction File™ (PDF®).
*© The Author(s), 2025. Published by Cambridge University Press on behalf of International Centre for Diffraction Data. This is an Open Access article, distributed under the terms of the Creative Commons Attribution licence (http://creativecommons.org/licenses/by/4.0), which permits unrestricted re-use, distribution and reproduction, provided the original article is properly cited.*
[doi:10.1017/S0885715625100936]

Key words: tafamidis, Vyndaqel, powder diffraction, Rietveld refinement, density functional theory

Tafamidis (sold under the brand names Vyndaqel and Vyndamax) is used to treat patients with heart disease by slowing nerve damage in adults diagnosed with polyneuropathy or cardiomyopathy. The systematic name (CAS Registry No. 594839-88-0) is 2-(3,5-dichlorophenyl)-1,3-benzoxazole-6-carboxylic acid. The crystal structures of Forms 1 and 4 of tafamidis have been reported just before this pattern was collected (Masciocchi et al., 2022). This work was carried out as part of a project (Kaduk et al., 2014) to determine the crystal structures of large-volume commercial pharmaceuticals and include high-quality room-temperature powder diffraction data for them in the Powder Diffraction File (Gates-Rector and Blanton, 2019).

Tafamidis was a commercial reagent, purchased from TargetMol (Batch #130404), and was used as received. The white powder was packed into a 1.5-mm-diameter Kapton capillary and rotated during the measurement at ~50 Hz. The powder pattern was measured at 295 K at beam line 11-BM (Antao et al., 2008; Lee et al., 2008; Wang et al., 2008) of the Advanced Photon Source at the Argonne National Laboratory using a wavelength of 0.459744(2) Å from 0.5 to 40° 2θ with a step size of 0.001° and a counting time of 0.1 sec/step (Figure 1). The high-resolution powder diffraction data were collected using 12 silicon crystal analyzers that allow for high angular resolution, high precision, and accurate peak positions. A mixture of silicon (NIST SRM 640c) and alumina (NIST SRM 676a) standards (ratio $Al_2O_3$:Si = 2:1 by weight) was used to calibrate the instrument and refine the monochromatic wavelength used in the experiment. The pattern was indexed using N-TREOR (Altomare et al., 2013) and solved using direct methods in EXPO2014. A reduced cell search in the Cambridge Structural Database (Groom et al., 2016) yielded the Refcode CEQDOV for tafamidis Form 1 (Masciocchi et al., 2022). The structure was refined using GSAS-II (Toby and Von Dreele, 2013) and optimized using VASP (Kresse and Furthmüller, 1996). A single-point density functional calculation (fixed experimental cell) and population analysis were carried out using CRYSTAL23 (Erba et al., 2022).

The crystal structure consists of stacks of molecules along the $a$-axis. The molecules are inclined to this axis; the mean plane is (−4, 2, 11). Strong centrosymmetric O–H···O hydrogen bonds (Table I) exist between carboxylic acid groups. The population analysis enabled the quantification of the strength of the O–H···O hydrogen bond using the correlation of Rammohan and Kaduk (2018). As noted by Masciocchi et al. (2022), the molecules are linked along the $b$-axis by C–H···N hydrogen bonds. Two C–H···Cl hydrogen bonds also contribute to the lattice energy. The overlap populations provide relative measures of the strengths of these C-donor hydrogen bonds.

The volume/non-H atom is smaller than usual, at 16.3 Å/atom, despite the presence of the two Cl atoms in the molecule. The Bravais–Friedel–Donnay–Harker (Bravais, 1866; Friedel, 1907; Donnay and Harker, 1937) algorithm suggests that we might expect needle morphology for tafamidis, with [100] as the long axis. A second-order spherical harmonic model was included in the refinement. The texture index was 1.017, indicating that the preferred orientation was slight in this rotated capillary specimen.

Corresponding author: James Kaduk; Email: kaduk@polycrystallography.com



https://doi.org/10.1017/S0885715625100936 Published online by Cambridge University Press

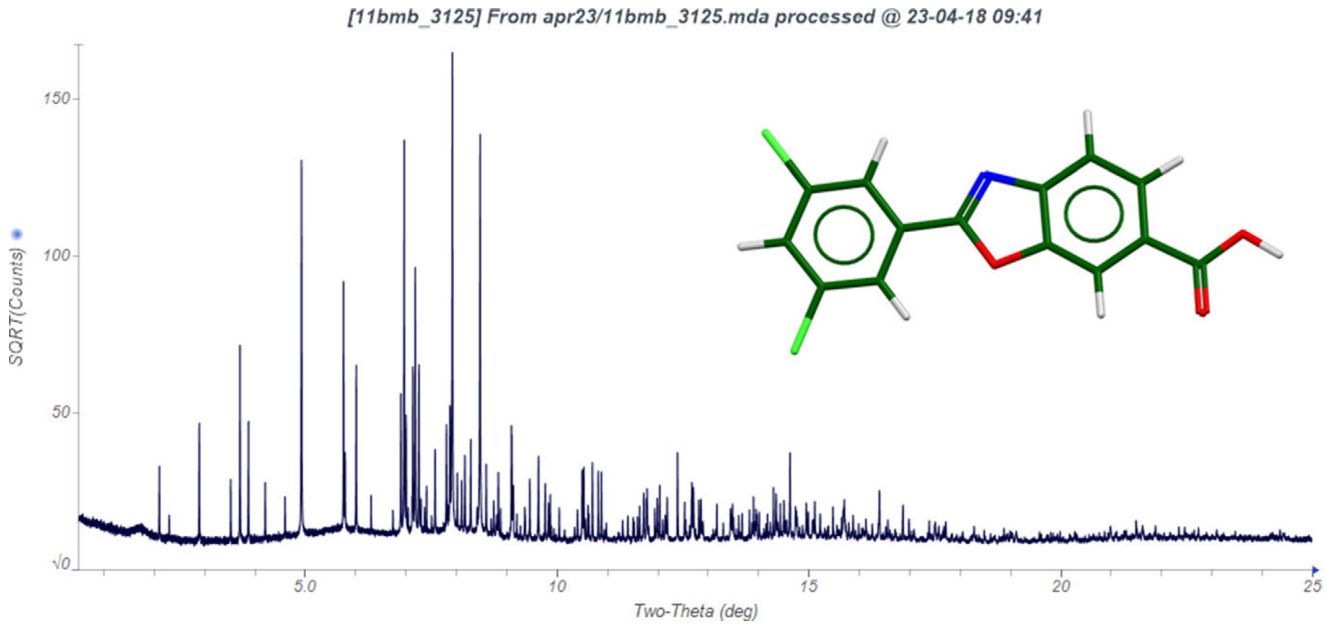



Figure 1. The synchrotron powder pattern of tafamidis (λ = 0.459744 Å), along with the molecular structure.

TABLE I. Hydrogen bonds (CRYSTAL23) in tafamidis Form 1

| H bond | D–H, Å | H···A, Å | D···A, Å | D–H···A, ° | Overlap, *e* | *E*, kcal/mol |
|---|---|---|---|---|---|---|
| O5–H21···O4 | 1.042 | 1.513 | 2.554 | 177.0 | 0.082 | 15.7 |
| C9–H22···Cl2 | 1.089 | 2.789 | 3.848 | 164.0 | 0.017 | |
| C12–H23···N6 | 1.091 | 2.414 | 3.482 | 165.8 | 0.024 | |
| C16–H25···Cl1 | 1.089 | 3.073 | 3.972 | 140.2 | 0.011 | |

## DEPOSITED DATA

The powder pattern of tafamidis Form 1 from this synchrotron dataset has been submitted to the International Centre for Diffraction Data (ICDD) for inclusion in the Powder Diffraction File. The Crystallographic Information Framework files containing the results of the Rietveld refinement (including the raw data) and the DFT geometry optimization were deposited with the ICDD. The data can be requested at pdj@icdd.com.


## ACKNOWLEDGEMENTS

We thank Saul Lapidus for his assistance in the data collection.

## FUNDING STATEMENT

The use of the Advanced Photon Source at the Argonne National Laboratory was supported by the U.S. Department of Energy, Office of Science, Office of Basic Energy Sciences, under Contract No. DE-AC02-06CH11357. This work was partially supported by the International Centre for Diffraction Data.


## CONFLICTS OF INTEREST

The authors have no conflicts of interest to declare.

## REFERENCES


Altomare, A., C. Cuocci, C. Giacovazzo, A. Moliterni, R. Rizzi, N. Corriero, and A. Falcicchio. 2013. "EXPO2013: A Kit of Tools for Phasing Crystal Structures from Powder Data." *Journal of Applied Crystallography* 46: 1231–1235. https://doi.org/10.1107/S0021889813013113.

Antao, S. M., I. Hassan, J. Wang, P. L. Lee, and B. H. Toby. 2008. "State-of-the-Art High-Resolution Powder X-Ray Diffraction (HRPXRD) Illustrated with Rietveld Refinement of Quartz, Sodalite, Tremolite, and Meionite." *Canadian Mineralogist* 46: 1501–9.

Bravais, A. 1866. *Etudes Cristallographiques*. Gauthier Villars.

Donnay, J. D. H., and D. Harker. 1937. "A New Law of Crystal Morphology Extending the Law of Bravais." *American Mineralogist* 22: 446–67.

Erba, A., J. K. Desmaris, S. Casassa, B. Civalleri, L. Donà, I. J. Bush, B. Searle, et al. 2022. "CRYSTAL23: A Program for Computational Solid State Physics and Chemistry." *Journal of Chemical Theory and Computation* 19: 6891–932. https://doi.org/10.1021/acs.jctc.2c00958.

Friedel, G. 1907. "Etudes sur la loi de Bravais." *Bulletin de la Société Française de Minéralogie* 30: 326–455.

Gates-Rector, S., and T. N. Blanton. 2019. "The Powder Diffraction File: A Quality Materials Characterization Database." *Powder Diffraction* 39: 352–60.

Groom, C. R., I. J. Bruno, M. P. Lightfoot, and S. C. Ward. 2016. "The Cambridge Structural Database." *Acta Crystallographica Section B: Structural Science, Crystal Engineering and Materials* 72: 171–79.

Kaduk, J. A., C. E. Crowder, K. Zhong, T. G. Fawcett, and M. R. Suchomel. 2014. "Crystal Structure of Atomoxetine Hydrochloride (Strattera), C17H22NOCl." *Powder Diffraction* 29: 269–273. https://doi.org/10.1017/S0885715614000517.

Kresse, G., and J. Furthmüller. 1996. "Efficiency of Ab-Initio Total Energy Calculations for Metals and Semiconductors Using a Plane-Wave Basis Set." *Computational Materials Science* 6: 15–50.




https://doi.org/10.1017/S0885715625100936 Published online by Cambridge University Press

Lee, P. L., D. Shu, M. Ramanathan, C. Preissner, J. Wang, M. A. Beno, R. B. Von Dreele, et al. 2008. "A Twelve-Analyzer Detector System for High-Resolution Powder Diffraction." *Journal of Synchrotron Radiation* 15: 427–32.

Masciocchi, N., V. M. Abbinate, M. Zambra, and G. Barreca. 2022. "Thermal and Structural Characterization of Two Crystalline Polymorphs of Tafamidis Free Acid." *Molecules* 27: 7411. https://doi.org/10.3390/molecules27217411.

Rammohan, Alagappa, and James A. Kaduk. 2018. "Crystal Structures of Alkali Metal (Group 1) Citrate Salts." *Acta Crystallographica Section B: Crystal Engineering and Materials* XX: 239–52. https://doi.org/10.1107/S2052520618002330.

Toby, B. H., and R. B. Von Dreele. 2013. "GSAS II: The Genesis of a Modern Open Source All Purpose Crystallography Software Package." *Journal of Applied Crystallography* 46: 544–49.

Wang, J., B. H. Toby, P. L. Lee, L. Ribaud, S. M. Antao, C. Kurtz, M. Ramanathan, R. B. Von Dreele, and M. A. Beno. 2008. "A Dedicated Powder Diffraction Beamline at the Advanced Photon Source: Commissioning and Early Operational Results." *Review of Scientific Instruments* 79: 085105. https://doi.org/10.1063/1.2969260.



https://doi.org/10.1017/S0885715625100936 Published online by Cambridge University Press